

A neutrino mass model with $S3$ symmetry and see-saw interplay

Soumita Pramanick*, Amitava Raychaudhuri†

Department of Physics, University of Calcutta, 92 Acharya Prafulla Chandra Road, Kolkata 700009, India

Abstract

We develop a see-saw model for neutrino masses and mixing with an $S3 \times Z3$ symmetry. It involves an interplay of Type-I and Type-II see-saw contributions of which the former is subdominant. The $S3 \times Z3$ quantum numbers of the fermion and scalar fields are chosen such that the Type-II see-saw generates a mass matrix which incorporates the atmospheric mass splitting and sets $\theta_{23} = \pi/4$. The solar splitting and θ_{13} are absent, while the third mixing angle can achieve any value, θ_{12}^0 . Specific choices of θ_{12}^0 are of interest, e.g., 35.3° (tribimaximal), 45.0° (bimaximal), 31.7° (golden ratio), and 0° (no solar mixing). The role of the Type-I see-saw is to nudge all the above into the range indicated by the data. The model results in novel interrelationships between these quantities due to their common origin, making it readily falsifiable. For example, normal (inverted) ordering is associated with θ_{23} in the first (second) octant. CP-violation is controlled by phases in the right-handed neutrino Majorana mass matrix, $M_{\nu R}$. In their absence, only normal ordering is admissible. When $M_{\nu R}$ is complex the Dirac CP-phase, δ , can be large, i.e., $\sim \pm\pi/2$, and inverted ordering is also allowed. The preliminary results from T2K and NOVA which favour normal ordering and $\delta \sim -\pi/2$ are indicative, in this model, of a lightest neutrino mass of 0.05 eV or more.

Key Words: Neutrino mixing, θ_{13} , Solar splitting, $S3$, see-saw, Leptonic CP-violation

I Introduction

Oscillation experiments over vastly different baselines and a range of neutrino energies have filled up a vast portion of the mass and mixing jigsaw of the neutrino sector. Yet, we still remain in the dark with regard to CP-violation in the lepton sector. Neither do we know the mass ordering – whether it is normal or inverted. Further open issues are the absolute mass scale of neutrinos and whether they are of Majorana or Dirac nature. While we await experimental guidance for each of the above unknowns, there have been many attempts to build models of lepton mass which capture much of what is known.

Here we propose a neutrino mass model based on the direct product group $S3 \times Z3$. The elements of $S3$ correspond to the permutations of three objects¹. Needless to say, $S3$ -based models of neutrino mass have been considered earlier [1, 2]. A popular point of view [3] has been to note that a permutation symmetry between the three neutrino states is consistent with² (a) a democratic mass matrix, M_{dem} , all whose elements are equal, and (b) a mass matrix proportional to the identity matrix, I . A general combination of these two forms, e.g., $c_1 I + c_2 M_{dem}$, where c_1, c_2 are complex numbers, provides a natural starting point. One of the eigenstates, namely, an equal weighted combination of the three states, is one

*email: soumitapramanick5@gmail.com

†email: palitprof@gmail.com

¹More details of $S3$ can be found in Appendix A.

²Note, however, there is no 3-dimensional irreducible representation of $S3$ (see Appendix A). So these models entail fine tuning.

Model	TBM	BM	GR	NSM
θ_{12}^0	35.3°	45.0°	31.7°	0.0°

Table 1: The solar mixing angle, θ_{12}^0 for this work, for the TBM, BM, and GR mixing patterns. NSM stands for the case where the solar mixing angle is initially vanishing.

column of the popular tribimaximal mixing matrix. Many models have been presented [3] which add perturbations to this structure to accomplish realistic neutrino masses and mixing. Variations on this theme [4] explore mass matrices with such a form in the context of Grand Unified Theories, in models of extra dimensions, and examine renormalisation group effects on such a pattern realised at a high energy. Other variants of the $S3$ -based models, for example [5], rely on a 3-3-1 local gauge symmetry, tie it to a $(B - L)$ -extended model, or realise specific forms of mass matrices through soft symmetry breaking, etc. As discussed later, the irreducible representations of $S3$ are one and two-dimensional. The latter provides a natural mechanism to get maximal mixing in the $\nu_\mu - \nu_\tau$ sector [6].

The present work, also based on $S3$ symmetry, breaks new ground in the following directions. Firstly, it involves an interplay of Type-I and Type-II see-saw contributions. Secondly, it presents a general framework encompassing many popular mixing patterns such as tribimaximal mixing. Further, the model does not invoke any soft symmetry breaking terms. All the symmetries are broken spontaneously.

We briefly outline here the strategy of this work. We use the standard notation for the leptonic mixing matrix – the Pontecorvo, Maki, Nakagawa, Sakata (PMNS) matrix – U .

$$U = \begin{pmatrix} c_{12}c_{13} & s_{12}c_{13} & s_{13}e^{-i\delta} \\ -c_{23}s_{12} + s_{23}s_{13}c_{12}e^{i\delta} & c_{23}c_{12} + s_{23}s_{13}s_{12}e^{i\delta} & s_{23}c_{13} \\ s_{23}s_{12} + c_{23}s_{13}c_{12}e^{i\delta} & -s_{23}c_{12} + c_{23}s_{13}s_{12}e^{i\delta} & c_{23}c_{13} \end{pmatrix}, \quad (1)$$

where $c_{ij} = \cos\theta_{ij}$ and $s_{ij} = \sin\theta_{ij}$. The neutrino masses and mixings arise through a two-stage mechanism. In the first step, from the Type-II see-saw the larger atmospheric mass splitting, Δm_{atmos}^2 , is generated while the solar splitting, Δm_{solar}^2 , is absent. Also, $\theta_{13} = 0$, $\theta_{23} = \pi/4$ and the model parameters can be continuously varied to obtain any desired θ_{12}^0 . Of course, in reality $\theta_{13} \neq 0$ [7], the solar splitting is non-zero, and there are indications that θ_{23} is large but non-maximal. Experiments have also set limits on θ_{12} . The Type-I see-saw addresses all the above issues and relates the masses and mixings to each other.

The starting form incorporates several well-studied mixing patterns such as tribimaximal (TBM), bi-maximal (BM), and golden ratio (GR) mixings within its fold. These alternatives all have $\theta_{13} = 0$ and $\theta_{23} = \pi/4$. They differ only in the value of the third mixing angle θ_{12}^0 as displayed in Table 1. The fourth option in this Table, no solar mixing (NSM), exhibits the attractive feature³ that the mixing angles are either maximal, i.e., $\pi/4$ (θ_{23}) or vanishing (θ_{13} and θ_{12}^0).

In the following section we furnish a description of the model including the assignment of $S3 \times Z3$ quantum numbers to the leptons and symmetry-breaking scalar fields. The consequences of the model are described next where we also compare with the experimental data. A summary and conclusions follow. The scalar potential of this model has a rich structure. In two Appendices we present the

³Such a mixing pattern was envisioned earlier in a model based on $A4$ symmetry [8] which built on previous work along similar lines [9, 10].

Fields	Notations	$S3$ ($Z3$)	$SU(2)_L(Y)$	L
Left-handed leptons	L_e L_μ L_τ	$1'$ (1) $1'$ (ω) 1 (ω)	2 (-1)	+1
Right-handed charged leptons	e_R $\begin{pmatrix} \mu_R \\ \tau_R \end{pmatrix}$	$1'$ (1) 2 (1)	1 (-2)	+1
Right-handed neutrinos	N_{1R} N_{2R} N_{3R}	$1'$ (1) $1'$ (ω) 1 (ω)	1 (0)	0

Table 2: *The fermion content of the model. The transformation properties under $S3$, $Z3$, and $SU(2)_L$ are shown. The hypercharge of the fields, Y , and their lepton number, L , are also indicated. Here $L_\alpha^T = (\nu_\alpha \ l_\alpha^-)$.*

essence of $S3$ symmetry and discuss the $S3$ invariant scalar potential, deriving the conditions which must be satisfied by the scalar coefficients to obtain the desired minimum.

II The Model

In the model under discussion fermion and scalar multiplets are assigned $S3 \times Z3$ quantum numbers in a manner such that spontaneous symmetry breaking naturally yields mass matrices which lead to the see-saw features espoused earlier. All terms allowed by the symmetries of the model are included in the Lagrangian. No soft symmetry-breaking terms are required.

To begin it will be useful to formulate the conceptual structure behind the model. Neutrino masses arise from a combination of Type-I and Type-II see-saw contributions of which the latter dominates. In the neutrino mass basis, which is also the basis in which the Lagrangian will be presented, the Type-II see-saw yields a diagonal matrix in which two states are degenerate:

$$M_{\nu L} = \begin{pmatrix} m_1^{(0)} & 0 & 0 \\ 0 & m_1^{(0)} & 0 \\ 0 & 0 & m_3^{(0)} \end{pmatrix}. \quad (2)$$

This mass matrix results in $\Delta m_{atmos}^2 = (m_3^{(0)})^2 - (m_1^{(0)})^2$ while $\Delta m_{solar}^2 = 0$. Later, we find the combinations $m^\pm = m_3^{(0)} \pm m_1^{(0)}$ useful. m^- signals the mass ordering; it is positive for normal ordering (NO) and negative for inverted ordering (IO).

At this stage the mixing resides entirely in the charged lepton sector. We follow the convention

$$\Psi_{flavour} = U\Psi_{mass} , \quad (3)$$

for the fermions Ψ , so that the PMNS matrix, U , is given by

$$U = U_l^\dagger U_\nu . \quad (4)$$

As noted, at this level $\theta_{12} = \theta_{12}^0$, where alternate choices of θ_{12}^0 result in popular mixing patterns such as tribimaximal, bimaximal, and golden ratio with the common feature that $\theta_{13} = 0$ and $\theta_{23} = \pi/4$. $\theta_{12}^0 = 0$ is another interesting alternative [8] where initially the lepton mixing angles are either vanishing $\theta_{13} = 0 = \theta_{12}$ or maximal, i.e., $\pi/4$ (θ_{23}). Thus, till Type-I see-saw effects are included, the leptonic mixing matrix takes the form:

$$U^0 = \begin{pmatrix} \cos \theta_{12}^0 & \sin \theta_{12}^0 & 0 \\ -\frac{\sin \theta_{12}^0}{\sqrt{2}} & \frac{\cos \theta_{12}^0}{\sqrt{2}} & \frac{1}{\sqrt{2}} \\ \frac{\sin \theta_{12}^0}{\sqrt{2}} & -\frac{\cos \theta_{12}^0}{\sqrt{2}} & \frac{1}{\sqrt{2}} \end{pmatrix} = U_l^\dagger U_\nu^0 , \quad (5)$$

where $U_\nu^0 = I$ and the charged lepton mass matrix is:

$$M_{e\mu\tau} = U_l \begin{pmatrix} m_e & 0 & 0 \\ 0 & m_\mu & 0 \\ 0 & 0 & m_\tau \end{pmatrix} I = \begin{pmatrix} m_e \cos \theta_{12}^0 & -\frac{m_\mu}{\sqrt{2}} \sin \theta_{12}^0 & \frac{m_\tau}{\sqrt{2}} \sin \theta_{12}^0 \\ m_e \sin \theta_{12}^0 & \frac{m_\mu}{\sqrt{2}} \cos \theta_{12}^0 & -\frac{m_\tau}{\sqrt{2}} \cos \theta_{12}^0 \\ 0 & \frac{m_\mu}{\sqrt{2}} & \frac{m_\tau}{\sqrt{2}} \end{pmatrix} . \quad (6)$$

The identity matrix, I , at the right in the first step above indicates that no transformation needs to be applied on the right-handed charged leptons which are $SU(2)_L$ singlets.

In this basis, the matrices responsible for the Type-I see-saw have the forms:

$$M_D = m_D \mathbb{I} \text{ and } M_{\nu R} = \frac{m_R}{2xy} \begin{pmatrix} 0 & xe^{-i\phi_1} & xe^{-i\phi_1} \\ xe^{-i\phi_1} & ye^{-i\phi_2}/\sqrt{2} & -ye^{-i\phi_2}/\sqrt{2} \\ xe^{-i\phi_1} & -ye^{-i\phi_2}/\sqrt{2} & ye^{-i\phi_2}/\sqrt{2} \end{pmatrix} , \quad (7)$$

where m_D and m_R set the scale for the Dirac and right-handed Majorana masses while x and y are dimensionless real quantities of $\mathcal{O}(1)$. We take the Dirac mass matrix M_D proportional to the identity for ease of presentation. We have checked that the same results can be reproduced so long as M_D is diagonal. The right-handed neutrino Majorana mass matrix, $M_{\nu R}$, has a $N_{2R} \leftrightarrow N_{3R}$ discrete symmetry. This choice too can be relaxed without jeopardising the final outcome.

We will show later how the mass matrices in eqs. (2) - (7) lead to a good fit to the neutrino data and yield testable predictions. But before this we must ensure that the above matrices can arise from the $S3 \times Z3$ symmetric Lagrangian.

The behaviour of the fermions, i.e., the three lepton generations⁴ including three right-handed neutrinos, is summarised in Table 2. The gauge interactions of the leptons are universal and diagonal in this basis. A feature worth noting is that the right-handed neutrinos have lepton number $L = 0$. We discuss later how this leads to a diagonal neutrino Dirac mass matrix. The lepton mass matrices arise from the Yukawa couplings allowed by the $S3 \times Z3$ symmetry.

⁴The scope of this model is restricted to the lepton sector.

Purpose	Notations	$S3$ ($Z3$)	$SU(2)_L$ (Y)	L	vev
Charged fermion mass	$\eta \equiv (\eta^+ \eta^0)$	1 (1)	2 (1)	0	$\langle \eta \rangle = v_\eta (0 \ 1)$
	$\Phi_a \equiv \begin{pmatrix} \phi_1^+ & \phi_1^0 \\ \phi_2^+ & \phi_2^0 \end{pmatrix}$	2 (1)	2 (1)	0	$\langle \Phi_a \rangle = \frac{v_a}{\sqrt{2}} \begin{pmatrix} 0 & w_1 \\ 0 & w_2 \end{pmatrix}$
	$\Phi_b \equiv \begin{pmatrix} \phi_3^+ & \phi_3^0 \\ \phi_4^+ & \phi_4^0 \end{pmatrix}$	2 (ω)	2 (1)	0	$\langle \Phi_b \rangle = \frac{v_b}{\sqrt{2}} \begin{pmatrix} 0 & w_3 \\ 0 & w_4 \end{pmatrix}$
	$\alpha \equiv (\alpha^+ \alpha^0)$	1 (ω)	2 (1)	0	$\langle \alpha \rangle = v_\alpha (0 \ 1)$
Neutrino Dirac mass	$\beta \equiv (\beta^0 \beta^-)$	1 (1)	2 (-1)	1	$\langle \beta \rangle = v_\beta (1 \ 0)$
Type-II see-saw mass	$\Delta_L \equiv (\Delta_L^{++}, \Delta_L^+, \Delta_L^0)$	1 (1)	3 (2)	-2	$\langle \Delta_L \rangle = v_\Delta (0 \ 0 \ 1)$
	$\rho_L \equiv (\rho_L^{++}, \rho_L^+, \rho_L^0)$	1 (ω)	3 (2)	-2	$\langle \rho_L \rangle = v_\rho (0 \ 0 \ 1)$
Right-handed neutrino mass	$\chi \equiv \chi^0$	1 (ω)	1 (0)	0	$\langle \chi \rangle = u_\chi$
	$\gamma \equiv \gamma^0$	1' (ω)	1 (0)	0	$\langle \gamma \rangle = u_\gamma$

Table 3: *The scalar content of the model. The transformation properties under $S3$, $Z3$, and $SU(2)_L$ are shown. The hypercharge of the fields, Y , their lepton number, L , and the vacuum expectation values are also indicated. w_i ($i = 1 \dots 4$) are dimensionless.*

The $S3 \times Z3$ structure of the lepton sector is matched by a rich scalar sector which we have presented in Table 3. The requirement of charged lepton masses and Type-I and Type-II see-saw neutrino masses dictates the inclusion of $SU(2)_L$ singlet, doublet, and triplet scalar fields. The $S3 \times Z3$ properties of the scalars are chosen bearing in mind the $S3$ and $Z3$ combination rules. In particular, for the former the representations are 1, 1', and 2 which satisfy the multiplication rules (see Appendix A):

$$1 \times 1' = 1' , \quad 1' \times 1' = 1 , \quad \text{and} \quad 2 \times 2 = 2 + 1 + 1' . \quad (8)$$

The scalar multiplets are chosen such that the mass matrices appear with specific structures as discussed below⁵. It can be seen from Table 3 that all neutral scalars pick up a vev . The vev of the $SU(2)_L$ singlets, namely, u_χ and u_γ , can be much higher than the electroweak scale, v , and determine the masses of the right-handed neutrinos. The other vev break $SU(2)_L$. We take $v_\Delta \sim v_\rho \ll v_\eta \sim v_a \sim v_b \sim v_\alpha \sim v_\beta \sim v$.

Charged lepton and neutrino masses are obtained from the Yukawa terms in a Lagrangian constructed

⁵In general the multiple scalar fields in models based on discrete symmetries also result in flavour changing neutral currents induced by the neutral scalars. Discussions of this aspect in the context of $S3$ can be found, for example, in [11].

out of the fields in Tables 2 and 3. Including all terms which respect the $SU(2)_L \times U(1)_Y$ gauge symmetry and the $S3 \times Z3$ flavour symmetry so long as lepton number, L , is also conserved one is led to the Lagrangian mass terms

$$\begin{aligned}
\mathcal{L}_{mass} &= f_1 \bar{e}_L(\mu_R\phi_2^0 - \tau_R\phi_1^0) + f_2 \bar{\mu}_L(\mu_R\phi_4^0 - \tau_R\phi_3^0) + f_3 \bar{\tau}_L(\mu_R\phi_4^0 + \tau_R\phi_3^0) \\
&+ f_4 \bar{\mu}_L e_R \alpha^0 + f_5 \bar{e}_L e_R \eta^0 \quad (\text{charged lepton mass}) \\
&+ (h_1 \bar{\nu}_{eL} N_{1R} + h_2 \bar{\nu}_{\mu L} N_{2R} + h_3 \bar{\nu}_{\tau L} N_{3R}) \beta^0 \quad (\text{neutrino Dirac mass}) \\
&+ \frac{1}{2} g_1 \nu_{eL}^T C^{-1} \nu_{eL} \Delta_L^0 + \frac{1}{2} (g_2 \nu_{\mu L}^T C^{-1} \nu_{\mu L} + g_3 \nu_{\tau L}^T C^{-1} \nu_{\tau L}) \rho_L \quad (\text{neutrino Type-II see-saw mass}) \\
&+ \frac{1}{2} ([k_1 N_{2R}^T C^{-1} N_{2R} + k_2 N_{3R}^T C^{-1} N_{3R}] \chi + k_3 N_{2R}^T C^{-1} N_{3R} \gamma) \\
&+ \frac{1}{2} (k_4 N_{1R}^T C^{-1} N_{2R} \tilde{\chi} + k_5 N_{1R}^T C^{-1} N_{3R} \tilde{\gamma}) \quad (\text{rh neutrino mass}) + h.c. \quad . \quad (9)
\end{aligned}$$

Here, $\tilde{\chi}$ and $\tilde{\gamma}$ are charge conjugated fields which transform under Z_3 as ω^2 . For each term in the Lagrangian the fermion masses which arise therefrom have been indicated. Both Type-I and Type-II see-saw contributions for neutrino masses are present.

The above Lagrangian gives rise to the mass matrices in Eqs. (2) - (7) through the Yukawa couplings in Eq. (9) and the $vevs$ in Table 3. Before turning to these let us note how the quantum number assignments of the fermion and scalar fields force certain entries in the mass matrices to be vanishing. For example, the mass term $\bar{\tau}_L e_R$ is zero in Eq. (6) because there is no $SU(2)_L$ doublet field which transforms as a $1'$ under $S3$. Similarly the diagonal nature of the left-handed neutrino Majorana mass matrix in Eq. (2) is ensured by the absence of an $SU(2)_L$ triplet field which transforms either as (i) a $1'$ under $S3$ or (ii) as ω^2 under Z_3 . The neutrino Dirac mass matrix in Eq. (7) arises from the Yukawa couplings⁶ of the $SU(2)_L$ doublet scalar β . Since it transforms as 1 under both $S3$ and $Z3$ it can be seen from the left-handed and right-handed neutrino quantum numbers in Table 2 that only diagonal terms are allowed. Finally, the $N_{1R}^T N_{1R}$ term is absent in the right-handed neutrino Majorana mass matrix in Eq. (7) since there is no $Z3$ singlet among the $SU(2)_L$ singlet scalars.

Before proceeding further it may be useful to comment on the sizes of the various vacuum expectation values in Table 3. The $SU(2)_L$ doublets acquire $vevs$ $v_{\eta,a,b,\alpha,\beta}$ which are $\mathcal{O}(M_W)$ while the triplet $vevs$ $v_{\Delta,\rho}$ are several orders of magnitude smaller. This is in consonance with the smallness of the neutrino masses as also the ρ parameter of electroweak symmetry breaking. Needless to say, the $SU(2)_L$ singlet fields χ and γ can acquire $vevs$ well above the electroweak scale.

The non-vanishing entries in the mass matrices in Eqs. (2) - (7) which arise from the Yukawa couplings entail the following relationships:

1. Charged lepton masses – On matching the Lagrangian in Eq. (9), the scalar doublet $vevs$ in Table 3 and the charged lepton mass matrix in Eq. (6) one gets:

$$f_1 \langle \phi_1^0 \rangle = -\frac{m_\tau}{\sqrt{2}} \sin \theta_{12}^0 \quad , \quad f_1 \langle \phi_2^0 \rangle = -\frac{m_\mu}{\sqrt{2}} \sin \theta_{12}^0 \quad , \quad (10)$$

$$f_2 \langle \phi_3^0 \rangle = \frac{m_\tau}{\sqrt{2}} \cos \theta_{12}^0 \quad , \quad f_2 \langle \phi_4^0 \rangle = \frac{m_\mu}{\sqrt{2}} \cos \theta_{12}^0 \quad , \quad f_3 \langle \phi_3^0 \rangle = \frac{m_\tau}{\sqrt{2}} \quad , \quad f_3 \langle \phi_4^0 \rangle = \frac{m_\mu}{\sqrt{2}} \quad , \quad (11)$$

⁶As the N_{iR} carry $L = 0$, conservation of lepton number forbids any contribution to the Dirac mass from the $SU(2)_L$ scalar doublets which generate the charged lepton masses.

and

$$f_4\langle\alpha^0\rangle = m_e \sin\theta_{12}^0, \quad f_5\langle\eta^0\rangle = m_e \cos\theta_{12}^0. \quad (12)$$

Notice that Eqs. (10) and (11) imply

$$\frac{w_2}{w_1} = \frac{w_4}{w_3} = \frac{m_\mu}{m_\tau}. \quad (13)$$

2. Left-handed neutrino Majorana mass – Similarly, the mass matrix in Eq. (2) is obtained when

$$g_1\langle\Delta_L^0\rangle = m_1^0 = g_2\langle\rho_L^0\rangle, \quad g_3\langle\rho_L^0\rangle = m_3^0. \quad (14)$$

The first equation above requires a matching between two sets of Yukawa couplings and *vevs*. This is to ensure degeneracy of two neutrino states, implying the vanishing of the solar mass splitting at this stage. Notice that the relatively large size of the atmospheric mass splitting requires g_2 and g_3 to be of different order.

3. Neutrino Dirac mass – The Dirac mass matrix in Eq. (7) is due to the relations:

$$h_1 = h_2 = h_3 = h \quad \text{and} \quad h\langle\beta^0\rangle = m_D. \quad (15)$$

The equality of the three Yukawa couplings, h_i , above is only a simplified choice. We have checked that deviations from this relation, i.e., a diagonal Dirac mass matrix but not proportional to the identity, can also readily lead to the results which we discuss in this paper.

4. Right-handed neutrino Majorana mass – Finally, the right-handed neutrino Majorana mass matrix follows from:

$$k_1\langle\chi^0\rangle = \frac{m_R e^{-i\phi_2}}{2\sqrt{2}x} = k_2\langle\chi^0\rangle, \quad k_3\langle\gamma^0\rangle = -\frac{m_R e^{-i\phi_2}}{2\sqrt{2}x}, \quad k_4\langle\tilde{\chi}^0\rangle = \frac{m_R e^{-i\phi_1}}{2y} = k_5\langle\tilde{\gamma}^0\rangle. \quad (16)$$

We show in Appendix B how from a minimisation of the scalar potential the required scalar *vevs* may be obtained.

II.1 Type-I see-saw contribution

In the previous section we have shown that the $S3$ model results in a diagonal left-handed neutrino mass matrix given in Eq. (2) through a Type-II see-saw. The charged lepton mass matrix as given in Eq. (6) is not diagonal and induces a mixing in the lepton sector. This mixing, Eq. (5), receives further corrections from a smaller Type-I see-saw contribution to the neutrino mass matrix as we discuss.

The Type-I see-saw arising from the Dirac and right-handed neutrino mass matrices in Eq. (7) is

$$M' = [M_D^T (M_{\nu R})^{-1} M_D] = \frac{m_D^2}{m_R} \begin{pmatrix} 0 & y e^{i\phi_1} & y e^{i\phi_1} \\ y e^{i\phi_1} & \frac{x e^{i\phi_2}}{\sqrt{2}} & \frac{-x e^{i\phi_2}}{\sqrt{2}} \\ y e^{i\phi_1} & \frac{-x e^{i\phi_2}}{\sqrt{2}} & \frac{x e^{i\phi_2}}{\sqrt{2}} \end{pmatrix}. \quad (17)$$

III Results

We have given above the contributions to the neutrino mass matrix from the Type-I and Type-II see-saw. Of these, the former is taken to be significantly smaller than the latter. As we have noted, in

the absence of the Type-I see-saw the leptonic mixing matrix in this model is determined entirely by the charged lepton mass matrix. It has $\theta_{13} = 0$, $\theta_{23} = \pi/4$, and θ_{12} arbitrary. We will be considering four mixing patterns which fall within this scheme and in each of which the value of θ_{12}^0 is specified, namely, the TBM, BM, GR, and NSM cases. In addition, in this model the Type-II see-saw sets the solar mass splitting to be zero. The Type-I see-saw, whose effect we incorporate perturbatively, brings all the above leptonic parameters into agreement with their values preferred by the data. Before we proceed further with this discussion it will be useful to summarise the global best-fit values of these mass-splittings and angles.

III.1 Data

From global fits the currently favoured 3σ ranges of the neutrino mixing parameters are [12, 13]

$$\begin{aligned}\Delta m_{21}^2 &= (7.02 - 8.08) \times 10^{-5} \text{ eV}^2, \quad \theta_{12} = (31.52 - 36.18)^\circ, \\ |\Delta m_{31}^2| &= (2.351 - 2.618) \times 10^{-3} \text{ eV}^2, \quad \theta_{23} = (38.6 - 53.1)^\circ, \\ \theta_{13} &= (7.86 - 9.11)^\circ, \quad \delta = (0 - 360)^\circ.\end{aligned}\tag{18}$$

These data are from NuFIT2.1 of 2016 [12]. Here, $\Delta m_{ij}^2 = m_i^2 - m_j^2$, so that $\Delta m_{31}^2 > 0$ (< 0) for normal (inverted) ordering. The data indicate two best-fit points for θ_{23} in the first and second octants. Later, we also remark about the compatibility of this model with the recent T2K and NOVA hints [14, 15] of δ being near $-\pi/2$.

III.2 Real $M_{\nu R}$ ($\phi_1 = 0$ or π , $\phi_2 = 0$ or π)

A limiting case, with less complications, corresponds to no CP-violation. This happens when $M_{\nu R}$ is real, i.e., the phases $\phi_{1,2}$ in Eq. (17) are 0 or π . These cases can be compactly considered by keeping x and y real but allowing them to be of either sign, i.e., four alternatives. We show below how the experimental data picks out one or the other out of these.

Without the phases $\phi_{1,2}$, i.e., for real $M_{\nu R}$, one gets

$$M' = \frac{m_D^2}{m_R} \begin{pmatrix} 0 & y & y \\ y & \frac{x}{\sqrt{2}} & -\frac{x}{\sqrt{2}} \\ y & -\frac{x}{\sqrt{2}} & \frac{x}{\sqrt{2}} \end{pmatrix}.\tag{19}$$

The equality of two neutrino masses from the Type-II see-saw requires the use of degenerate perturbation theory to obtain corrections to the solar mixing parameters. The 2×2 submatrix of M' relevant for this is:

$$M'_{2 \times 2} = \frac{m_D^2}{m_R} \begin{pmatrix} 0 & y \\ y & x/\sqrt{2} \end{pmatrix}.\tag{20}$$

This results in:

$$\theta_{12} = \theta_{12}^0 + \zeta, \quad \tan 2\zeta = 2\sqrt{2} \left(\frac{y}{x} \right).\tag{21}$$

A related quantity, ϵ , which is found useful later is given by

$$\sin \epsilon = \frac{y}{\sqrt{y^2 + x^2/2}} \quad \text{and} \quad \cos \epsilon = \frac{x/\sqrt{2}}{\sqrt{y^2 + x^2/2}}, \quad \text{i.e.,} \quad \tan \epsilon = \frac{1}{2} \tan 2\zeta.\tag{22}$$

Model (θ_{12}^0)	TBM (35.3°)	BM (45.0°)	GR (31.7°)	NSM (0.0°)
ζ	$-4.0^\circ \leftrightarrow 0.6^\circ$	$-13.7^\circ \leftrightarrow -9.1^\circ$	$-0.4^\circ \leftrightarrow 4.2^\circ$	$31.3^\circ \leftrightarrow 35.9^\circ$
ϵ	$-4.0^\circ \leftrightarrow 0.6^\circ$	$-14.5^\circ \leftrightarrow -9.3^\circ$	$-0.4^\circ \leftrightarrow 4.2^\circ$	$44.0^\circ \leftrightarrow 56.7^\circ$
$\epsilon - \theta_{12}^0$	$-39.2^\circ \leftrightarrow -34.6^\circ$	$-59.5^\circ \leftrightarrow -54.4^\circ$	$-39.2^\circ \leftrightarrow -30.0^\circ$	$44.0^\circ \leftrightarrow 56.7^\circ$

Table 4: The ranges of ζ (Eq. (21)), ϵ (Eq. (22)), and $(\epsilon - \theta_{12}^0)$ allowed by the data for the different popular mixing patterns.

Once a mixing pattern is chosen, i.e., θ_{12}^0 fixed, the experimental limits on θ_{12} as given in Eq. (18) set bounds on the range of ζ and also from Eq. (22) on ϵ . These are displayed for the four mixing patterns in Table 4. If ζ is positive (negative) then the ratio (y/x) will also be positive (negative). In addition, from Eq. (22) the sign of y is fixed by the value of ϵ . Taking these points into account one can conclude that x is always positive, i.e., ϕ_2 has to be 0, while y must be positive, $\phi_1 = 0$ (negative, $\phi_1 = \pi$) for NSM (BM). For the other mixing patterns, i.e., TBM and GR, both signs of y are possible.

The solar mass splitting arising from the Type-I see-saw is also obtained from Eq. (20).

$$\Delta m_{solar}^2 = \frac{\sqrt{2}m_D^2}{m_R} m_1^{(0)} \sqrt{x^2 + 8y^2} = \frac{\sqrt{2}m_D^2}{m_R} m_1^{(0)} \frac{x}{\cos 2\zeta} . \quad (23)$$

Furthermore, incorporating the leading order corrections to neutrino mixing from Eq. (19) one gets from Eq. (4):

$$U = U^0 U_\nu \text{ with } U_\nu = \begin{pmatrix} \cos \zeta & -\sin \zeta & \kappa_r \sin \epsilon \\ \sin \zeta & \cos \zeta & -\kappa_r \cos \epsilon \\ \kappa_r \sin(\zeta - \epsilon) & \kappa_r \cos(\zeta - \epsilon) & 1 \end{pmatrix} , \quad (24)$$

with

$$\kappa_r \equiv \frac{m_D^2}{m_R m^-} \sqrt{y^2 + x^2/2} = \frac{m_D^2}{m_R m^-} \frac{x}{\sqrt{2} \cos \epsilon} . \quad (25)$$

The third column of the leptonic mixing matrix becomes:

$$|\psi_3\rangle = \begin{pmatrix} \kappa_r \sin(\epsilon - \theta_{12}^0) \\ \frac{1}{\sqrt{2}}[1 - \kappa_r \cos(\epsilon - \theta_{12}^0)] \\ \frac{1}{\sqrt{2}}[1 + \kappa_r \cos(\epsilon - \theta_{12}^0)] \end{pmatrix} . \quad (26)$$

Since, as noted, x is always positive, κ_r is positive (negative) for normal (inverted) ordering.

The right-hand-side of Eq. (26) has to be matched with the third column of eq. (1). This yields:

$$\sin \theta_{13} \cos \delta = \kappa_r \sin(\epsilon - \theta_{12}^0) , \quad (27)$$

and

$$\tan(\pi/4 - \theta_{23}) \equiv \tan \omega = \kappa_r \cos(\epsilon - \theta_{12}^0) . \quad (28)$$

For ready reference, the ranges of $(\epsilon - \theta_{12}^0)$ allowed for the different mixing patterns are presented in Table 4. For normal ordering⁷ the CP-phase δ is 0 (π) when $\sin(\epsilon - \theta_{12}^0)$ is positive (negative). From Table 4 one can then observe that $\delta = 0$ for the NSM mixing pattern and is π for the three other cases. Needless to say, both correspond to CP-conservation.

⁷We show in the following that inverted ordering is not consistent with real $M_{\nu R}$.

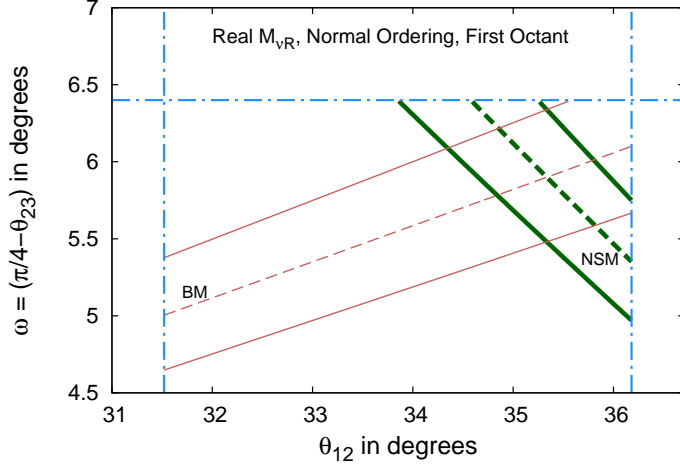


Figure 1: $\omega = (\pi/4 - \theta_{23})$ as a function of θ_{12} for normal ordering. The solid lines indicate the range for the 3σ allowed variation of $\sin \theta_{13}$ while the dashed line corresponds to the best-fit value. Thick green (thin pink) lines are for the NSM (BM) case. The horizontal and vertical blue dot-dashed lines delimit the 3σ allowed range from data. Note that ω is always positive, i.e., the first octant of θ_{23} is preferred. For the TBM and GR mixing patterns ω , still positive, lies beyond the 3σ range. Best-fit values of the solar and atmospheric splittings are used. For $M_{\nu R}$ real there is no allowed solution for inverted ordering.

Combining Eqs. (23), (25), and (27) one can write:

$$\Delta m_{solar}^2 = 2 m^- m_1^{(0)} \frac{\sin \theta_{13} \cos \delta \cos \epsilon}{\cos 2\zeta \sin(\epsilon - \theta_{12}^0)} . \quad (29)$$

Eq. (29) leads to the conclusion that inverted ordering is not allowed for this case of real $M_{\nu R}$. To establish this property one can define:

$$z \equiv m^- m_1^{(0)} / \Delta m_{atmos}^2 \quad \text{and} \quad \tan \xi \equiv m_0 / \sqrt{|\Delta m_{atmos}^2|} , \quad (30)$$

where z is positive for both mass orderings. From Eq. (29) one has

$$z = \left(\frac{\Delta m_{solar}^2}{|\Delta m_{atmos}^2|} \right) \left(\frac{\cos 2\zeta \sin(\epsilon - \theta_{12}^0)}{2 \sin \theta_{13} |\cos \delta| \cos \epsilon} \right) . \quad (31)$$

It is easy to verify from Eq. (30) that

$$\begin{aligned} z &= \sin \xi / (1 + \sin \xi) \quad \text{i.e.,} \quad 0 \leq z \leq \frac{1}{2} \quad (\text{for normal ordering}), \\ z &= 1 / (1 + \sin \xi) \quad \text{i.e.,} \quad \frac{1}{2} \leq z \leq 1 \quad (\text{for inverted ordering}) . \end{aligned} \quad (32)$$

There is a one-to-one correspondence of z with the lightest neutrino mass m_0 . The quasi-degeneracy limit, i.e., $m_0 \rightarrow \text{large}$, is approached as $z \rightarrow \frac{1}{2}$ for both mass orderings.

In Eq. (31) $|\cos \delta| = 1$ for real $M_{\nu R}$. Using the global fit mass splittings and mixing angles given in Sec. III.1 and Table 4 one finds $z \sim 10^{-2}$ or smaller for all four mixing patterns. This excludes the inverted mass ordering option for real $M_{\nu R}$.

From Eqs. (27) and (28) one has

$$\tan \omega = \frac{\sin \theta_{13} \cos \delta}{\tan(\epsilon - \theta_{12}^0)}. \quad (33)$$

The noteworthy point is that for normal ordering Eq. (28) implies that ω is always positive irrespective of the mixing pattern. So, in this model θ_{23} is restricted to the first octant only for real $M_{\nu R}$.

Eqs. (21) and (22) can be used to express ϵ in terms of θ_{12} and thereby put ω in Eq. (33) as a function of θ_{12} and θ_{13} only. In Fig. 1, ω is shown as a function of θ_{12} for the NSM (thick green lines) and BM (thin pink lines) mixing patterns. The ranges of θ_{12} and ω have been kept within their 3σ allowed limits from global fits as given in Sec. III.1. The TBM and GR cases are excluded because for the allowed values of θ_{12} they predict θ_{23} beyond the 3σ range. The solid lines in the figure correspond to the 3σ limiting values of θ_{13} and the dashed line is for its best-fit value. The blue dot-dashed horizontal and vertical lines display the 3σ experimental bounds on θ_{23} and θ_{12} .

Using Eq. (31) any allowed point in the $\omega - \theta_{12}$ plane and the associated θ_{13} can be translated to a value of z or equivalently m_0 , provided the solar and atmospheric mass splittings are given. We find that for both the allowed mixing patterns the range of variation of m_0 is very small. For the NSM (BM) case this range is $2.13 \text{ meV} \leq m_0 \leq 3.10 \text{ meV}$ ($3.20 \text{ meV} \leq m_0 \leq 4.42 \text{ meV}$) when both neutrino mass splittings and all mixing angles are varied over their full 3σ ranges.

To summarise the real $M_{\nu R}$ case:

1. Only the normal mass ordering is allowed.
2. θ_{23} can lie only in the first octant.
3. The TBM and GR alternatives are inconsistent with the allowed ranges of the neutrino mixing angles even after including the Type-I see-saw corrections.
4. For the NSM and BM mixing patterns real $M_{\nu R}$ can give consistent solutions for the neutrino masses and mixings. The ranges of allowed lightest neutrino masses are very tiny.

III.3 Complex $M_{\nu R}$

Keeping $M_{\nu R}$ real eliminates CP-violation. Further, inverted ordering is disallowed. Also, the TBM and GR mixing patterns cannot be accommodated. These restrictions can be ameliorated by taking $M_{\nu R}$ in its general complex form giving rise to the Type-I see-saw contribution M' as given in Eq. (17). Recall that this introduces the phases $\phi_{1,2}$ and x and y take only positive values.

With its complex entries, M' is now not hermitian any more. To address this we consider the combination $(M^0 + M')^\dagger(M^0 + M')$, and treat $M^{0\dagger}M^0$ as the leading term with $(M^{0\dagger}M' + M'^\dagger M^0)$ acting as a perturbation at the lowest order, both hermitian by construction. The unperturbed eigenvalues

are thus $(m_i^{(0)})^2$. The perturbation matrix is

$$(M^{0\dagger} M' + M'^{\dagger} M^0) = \frac{m_D^2}{m_R} \begin{pmatrix} 0 & 2ym_1^{(0)} \cos \phi_1 & yf(\phi_1) \\ 2ym_1^{(0)} \cos \phi_1 & \sqrt{2}xm_1^{(0)} \cos \phi_2 & -\frac{x}{\sqrt{2}}f(\phi_2) \\ yf^*(\phi_1) & -\frac{x}{\sqrt{2}}f^*(\phi_2) & \sqrt{2}xm_3^{(0)} \cos \phi_2 \end{pmatrix}. \quad (34)$$

In the above

$$f(\varphi) = m^+ \cos \varphi - im^- \sin \varphi. \quad (35)$$

The remaining calculation proceeds in much the same manner as for real $M_{\nu R}$ while keeping the distinctive features of Eq. (34) in mind.

In place of Eqs. (21) and (22) for the real $M_{\nu R}$ case, we get from (34)

$$\theta_{12} = \theta_{12}^0 + \zeta, \quad \tan 2\zeta = 2\sqrt{2} \frac{y}{x} \frac{\cos \phi_1}{\cos \phi_2}, \quad (36)$$

and

$$\sin \epsilon = \frac{y \cos \phi_1}{\sqrt{y^2 \cos^2 \phi_1 + x^2 \cos^2 \phi_2/2}}, \quad \cos \epsilon = \frac{x \cos \phi_2/\sqrt{2}}{\sqrt{y^2 \cos^2 \phi_1 + x^2 \cos^2 \phi_2/2}}, \quad \tan \epsilon = \frac{1}{2} \tan 2\zeta. \quad (37)$$

Mixing Pattern	Normal Ordering		Inverted Ordering	
	δ quadrant	θ_{23} octant	δ quadrant	θ_{23} octant
NSM	First/Fourth	First	Second/Third	Second
BM, TBM, GR	Second/Third	First	First/Fourth	Second

Table 5: *Quadrants of the leptonic CP-phase δ and the octant of θ_{23} for both mass orderings for different mixing patterns.*

The allowed ranges of ζ and ϵ depend on the mixing pattern and are given in Table 4. It is seen that for all patterns $\cos \epsilon$ is positive. Therefore, from Eq. (37) we can immediately conclude that ϕ_2 must be always in the first or fourth quadrants. The possible quadrants of ϕ_1 are also determined from the range of ϵ for the different mixing patterns. From the first relation in Eq. (37) we find that ϕ_1 has to be in the first or fourth (second or third) quadrants if ϵ is positive (negative). Using the results in Table 4 we conclude that the first (second) option is valid for the NSM (BM) patterns. For TBM and GR cases ϵ spans a range over positive and negative values and so both options are included.

The solar mass splitting is induced entirely through the Type-I see-saw contribution. From Eq. (34) one finds:

$$\Delta m_{solar}^2 = \sqrt{2}m_1^{(0)} \frac{m_D^2}{m_R} \sqrt{x^2 \cos^2 \phi_2 + 8y^2 \cos^2 \phi_1} = \sqrt{2}m_1^{(0)} \frac{m_D^2}{m_R} \frac{x \cos \phi_2}{\cos 2\zeta} = \sqrt{2}m_1^{(0)} \frac{m_D^2}{m_R} \frac{2\sqrt{2}y \cos \phi_1}{\sin 2\zeta}. \quad (38)$$

Eq. (26) is now replaced by:

$$|\psi_3\rangle = \begin{pmatrix} \kappa_c [\frac{\sin \epsilon}{\cos \phi_1} f(\phi_1) \cos \theta_{12}^0 - \frac{\cos \epsilon}{\cos \phi_2} f(\phi_2) \sin \theta_{12}^0] / m^+ \\ \frac{1}{\sqrt{2}} \{1 - \kappa_c [\frac{\sin \epsilon}{\cos \phi_1} f(\phi_1) \sin \theta_{12}^0 + \frac{\cos \epsilon}{\cos \phi_2} f(\phi_2) \cos \theta_{12}^0] / m^+\} \\ \frac{1}{\sqrt{2}} \{1 + \kappa_c [\frac{\sin \epsilon}{\cos \phi_1} f(\phi_1) \sin \theta_{12}^0 + \frac{\cos \epsilon}{\cos \phi_2} f(\phi_2) \cos \theta_{12}^0] / m^+\} \end{pmatrix}, \quad (39)$$

where

$$\kappa_c = \frac{m_D^2}{m_R m^-} \sqrt{y^2 \cos^2 \phi_1 + x^2 \cos^2 \phi_2 / 2}, \quad (40)$$

Eq. (37) has been used, and the complex function $f(\phi_{1,2})$ is defined in Eq. (35).

κ_c is positive (negative) for normal (inverted) ordering. Comparing the right-hand-side of Eq. (39) with the third column of Eq. (1) we find

$$\sin \theta_{13} \cos \delta = \kappa_c \sin(\epsilon - \theta_{12}^0), \quad (41)$$

$$\sin \theta_{13} \sin \delta = \kappa_c \frac{m^-}{m^+ \cos \phi_1 \cos \phi_2} \left[\sin \epsilon \sin \phi_1 \cos \phi_2 \cos \theta_{12}^0 - \cos \epsilon \cos \phi_1 \sin \phi_2 \sin \theta_{12}^0 \right]. \quad (42)$$

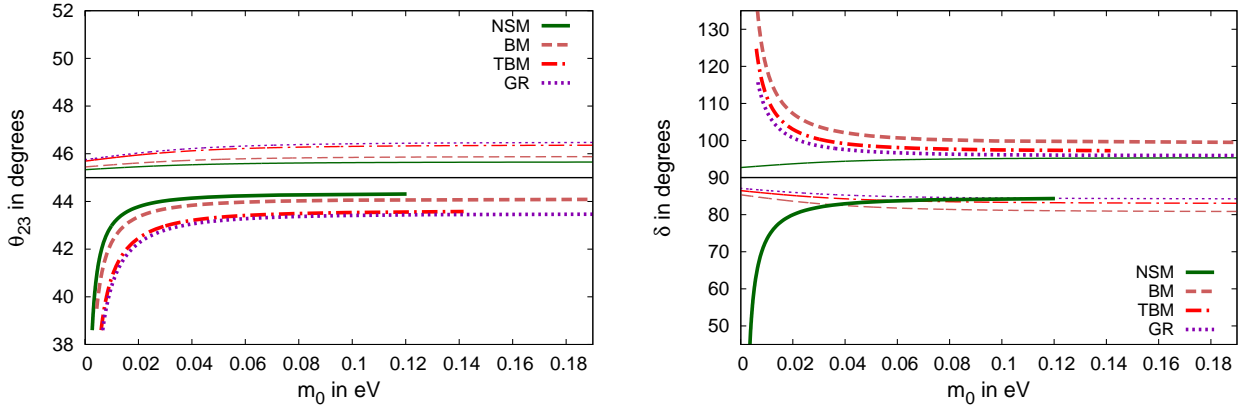


Figure 2: θ_{23} (left) and the CP-phase δ (right) as a function of m_0 from this model for different mixing patterns when the best-fit values of the input data are used. The NSM, BM, TBM and GR cases correspond to the green solid, pink dashed, red dot-dashed, and violet dotted curves respectively. Thick (thin) curves of each type indicate normal (inverted) mass orderings.

As indicated in Table 4, $(\epsilon - \theta_{12}^0)$ always remains in the first (fourth) quadrant for the NSM (BM, TBM, and GR) mixing pattern. For normal ordering Eq. (41) then implies that for the NSM (BM, TBM, and GR) case(s) δ lies in the first or fourth (second or third) quadrants. For inverted ordering of masses, κ_c changes sign and so the quadrants are accordingly modified. The different possibilities are indicated in Table 5. For any mixing pattern and mass ordering there are two allowed quadrants of δ which have $\sin \delta$ of opposite sign. Which of these is chosen is determined by the phases $\phi_{1,2}$ through the sign of the right-hand-side of Eq. (42). As noted above, ϕ_2 can be in either the first or fourth quadrants and the quadrant of ϕ_1 is determined by the mixing pattern in such a way that $\sin \phi_1$ can be of either sign. Thus the the phases ϕ_1 and ϕ_2 can always be chosen such that $\sin \delta$ can be of any particular sign. Therefore the two alternate quadrants of δ for every case in Table 5 are equally viable in this model.

The perturbative Type-I see-saw contribution to θ_{23} can also be extracted from Eq. (39). One finds:

$$\tan \omega = \frac{\sin \theta_{13} \cos \delta}{\tan(\epsilon - \theta_{12}^0)}. \quad (43)$$

Recalling that Eq. (41) correlates δ and $(\epsilon - \theta_{12}^0)$ through κ_c one can readily conclude that for all mixing patterns θ_{23} always lies in the first (second) octant for normal (inverted) ordering. This important conclusion from these models is shown in Table 5.

In the expression for the solar mass splitting in Eq. (38) one can trade the factor m_D^2/m_R in terms of κ_c and use Eq. (41) to get

$$\Delta m_{solar}^2 = \frac{2m^- m_1^{(0)} \sin \theta_{13} \cos \delta \cos \epsilon}{\sin(\epsilon - \theta_{12}^0) \cos 2\zeta}. \quad (44)$$

The strategy that we have followed to extract the predictions of this model relies on utilising Eqs. (43) and (44). We take the three mixing angles θ_{13} , θ_{12} , and θ_{23} as inputs. With these at hand Eq. (43) fixes a value of the CP-phase δ . Using these and the experimentally determined solar mass splitting one can calculate from Eq. (44) the combination $m_1^{(0)} m^-$, or equivalently the variable z , which fixes the lightest neutrino mass m_0 . It might appear that arbitrarily large values of m_0 , and hence $m_1^{(0)} m^-$, may be admitted by taking $\cos \delta$ to smaller and smaller values. However, this is not the case. Experimental data require $\omega = (\pi/4 - \theta_{23})$ to lie within determined limits. Since all other factors have experimentally allowed ranges, Eq. (43) also gives lower and upper bounds on δ . Consequently, for any mixing pattern m_0 lies within a fixed range.

In the left (right) panel of Fig. 2 we show the mixing angle θ_{23} (the CP phase δ) as a function of the lightest neutrino mass m_0 as obtained from this model for different mixing patterns when the best-fit values of the various measured angles and mass splittings are used. The NSM, BM, TBM and GR correspond to the green solid, pink dashed, red dot-dashed, and violet dotted curves respectively. The thick (thin) curves of each type indicate normal (inverted) mass orderings. Note that normal and inverted orderings are always associated with the first and second octants of θ_{23} respectively. For normal (inverted) ordering with the NSM mixing pattern δ lies in the first (second) quadrant while for the other cases it is in the second (first) quadrant. As expected, for inverted ordering $|\delta|$ stays close to $\pi/2$ for the entire range of m_0 . For normal ordering δ is near $\pi/2$ for m_0 larger than around 0.05 eV.

Of course, as indicated in Table 5 if δ is a solution for some m_0 then by suitably picking alternate values of the phases $\phi_{1,2}$ which appear in $M_{\nu R}$ one can also get a second solution with the phase $-\delta$. We have not shown this mirror set of solutions in Fig. 2. The T2K [14] and NOVA [15] experiments have presented data which may be taken as a preliminary hint of normal ordering associated with $\delta \sim -\pi/2$. As seen from Fig. 2 this is consistent with our model, with $\delta \sim -\pi/2$ favouring m_0 in the quasi-degenerate regime, i.e., $m_0 \geq \mathcal{O}(0.05 \text{ eV})$, for normal ordering. If this result is confirmed by further analysis then the model will require neutrino masses to be in a range to which ongoing experiments will be sensitive [16, 17].

The correlation between the octant of θ_{23} , the quadrant of the CP-phase δ , and the ordering of neutrino masses is a smoking-gun signal of this $S3 \times Z3$ based model.

IV Conclusions

In this paper we have put forward an $S3 \times Z3$ model for neutrino mass and mixing. After assigning the flavour quantum numbers to the leptons and the scalars we write down the most general Lagrangian consistent with the symmetry. Once the symmetry is broken, the Yukawa couplings give rise to the

charged lepton masses as well as the Dirac and Majorana masses for the left- and right-handed neutrinos. Neutrino masses originate from both Type-I and Type-II see-saw terms of which the former can be treated as a small correction. The dominant Type-II see-saw results in the atmospheric mass splitting, no solar splitting, keeps $\theta_{23} = \pi/4$, and $\theta_{13} = 0$. By a choice of the Yukawa couplings θ_{12} can be given any preferred value. Thus, at this level this model can accommodate any of the much-studied tribimaximal, bimaximal, golden ratio, and ‘no solar mixing’ patterns. The smaller Type-I see-saw contribution acting as a perturbation generates the solar mass splitting and nudges the mixing angles to values consistent with the global fits. The octants of θ_{23} are correlated with the neutrino mass ordering – first (second) octant is allowed for normal (inverted) ordering. The model is testable through its predictions for the CP-phase δ and from the relationships between mixing angles and mass splittings that it entails. Further, inverted mass ordering is correlated with a near-maximal CP-phase δ and arbitrarily small neutrino masses are permitted. For normal mass ordering δ can vary over a wider range and maximality is realised in the quasi-degenerate limit. The lightest neutrino mass must be at least a few meV in this case.

Acknowledgements: SP acknowledges support from CSIR, India. AR is partially funded by SERB Grant No. SR/S2/JCB-14/2009.

A Appendix: Essentials of the S_3 group

S_3 is a discrete group of order 6 which consists of all permutations of three objects. It can be generated by two elements A and B satisfying $A^2 = I = B^3$ and $(AB)^3 = I$. The group table is given below.

	I	A	B	C	D	F
I	I	A	B	C	D	F
A	A	I	C	B	F	D
F	F	C	I	D	A	B
C	C	F	D	I	B	A
D	D	B	A	F	I	C
B	B	D	F	A	C	I

Table 6: *The group table for S_3 .*

The group has two 1-dimensional representations denoted by 1 and $1'$, and a 2-dimensional representation. 1 is inert under the group while $1'$ changes sign under the action of A . For the 2-dimensional representation a suitable choice of matrices with the specified properties can be readily obtained. We choose

$$I = \begin{pmatrix} 1 & 0 \\ 0 & 1 \end{pmatrix}, \quad A = \begin{pmatrix} 0 & 1 \\ 1 & 0 \end{pmatrix}, \quad B = \begin{pmatrix} \omega & 0 \\ 0 & \omega^2 \end{pmatrix}, \quad (\text{A.1})$$

where ω is a cube root of unity, i.e., $\omega = e^{2\pi i/3}$. For this choice of A and B the remaining matrices of the representation are:

$$C = \begin{pmatrix} 0 & \omega^2 \\ \omega & 0 \end{pmatrix}, \quad D = \begin{pmatrix} 0 & \omega \\ \omega^2 & 0 \end{pmatrix}, \quad F = \begin{pmatrix} \omega^2 & 0 \\ 0 & \omega \end{pmatrix}. \quad (\text{A.2})$$

The product rules for the different representations are:

$$1 \times 1' = 1', \quad 1' \times 1' = 1, \quad \text{and} \quad 2 \times 2 = 2 + 1 + 1'. \quad (\text{A.3})$$

One can see that each of the 2×2 matrices M_{ij} in eqs. (A.1) and (A.2) satisfies:

$$\sum_{j,l=1,2} \alpha_{jl} M_{ij} M_{kl} = \alpha_{ik} \quad , \quad (\text{A.4})$$

where $\alpha_{ij} = 0$ for $i = j$ and $\alpha_{ij} = 1$ for $i \neq j$.

If $\Phi \equiv \begin{pmatrix} \phi_1 \\ \phi_2 \end{pmatrix}$ and $\Psi \equiv \begin{pmatrix} \psi_1 \\ \psi_2 \end{pmatrix}$ are two field multiplets transforming under $S3$ as doublets then using eqs. (A.1) and (A.4):

$$\phi_1 \psi_2 + \phi_2 \psi_1 \equiv 1 \quad , \quad \phi_1 \psi_2 - \phi_2 \psi_1 \equiv 1' \quad \text{and} \quad \begin{pmatrix} \phi_2 \psi_2 \\ \phi_1 \psi_1 \end{pmatrix} \equiv 2 \quad . \quad (\text{A.5})$$

Sometimes we have to deal with hermitian conjugate fields. Noting the nature of the complex representation (see, for example, B in eq. (A.1)) the conjugate $S3$ doublet is $\Phi^\dagger \equiv \begin{pmatrix} \phi_2^\dagger \\ \phi_1^\dagger \end{pmatrix}$. As a result, one has in place of (A.5)

$$\phi_2^\dagger \psi_2 + \phi_1^\dagger \psi_1 \equiv 1 \quad , \quad \phi_2^\dagger \psi_2 - \phi_1^\dagger \psi_1 \equiv 1' \quad \text{and} \quad \begin{pmatrix} \phi_1^\dagger \psi_2 \\ \phi_2^\dagger \psi_1 \end{pmatrix} \equiv 2 \quad . \quad (\text{A.6})$$

Eqs. (A.5) and (A.6) are essential in writing down the fermion mass matrices in Sec. II.

B Appendix: The scalar potential and its minimum

As seen in Table 3 this model has a rich scalar field content. In this Appendix we write down the scalar potential of the model keeping all these fields and derive conditions which must be met by the coefficients of the various terms so that the desired *vevs* can be achieved. These conditions ensure that the potential is locally minimized by this choice.

Table 3 displays the behaviour of the scalar fields under $S3 \times Z3$ besides the gauged electroweak $SU(2)_L \times U(1)_Y$. The fields also carry a lepton number. The scalar potential is the most general polynomial in these fields with up to quartic terms. Our first step will be to write down the explicit form of this potential. Here we do not exclude any term permitted by the symmetries. $SU(2)_L \times U(1)_Y$ invariance of the terms as well as the abelian lepton number and $Z3$ conservation are readily verified. It is only the $S3$ behaviour which merits special attention.

There are a variety of scalar fields in this model, e.g., $SU(2)_L$ singlets, doublets, and triplets. Therefore, the scalar potential has a large number of terms. For simplicity we choose all couplings in the potential to be real. In this Appendix we list the potential in separate parts: (a) those belonging to any one $SU(2)_L$ sector, and (b) inter-sector couplings of scalars. The $SU(2)_L$ singlet *vevs*, which are responsible for the right-handed neutrino mass, are significantly larger than those of other scalars. So, in the second category we retain only those terms which couple the singlet fields to either the doublet or the triplet sectors.

B.1 $SU(2)_L$ Singlet Sector:

The $SU(2)_L$ singlet sector comprises of two fields χ and γ transforming as $1(\omega)$ and $1'(\omega)$ of $S3$ (Z_3) respectively. They have $L = 0$. The scalar potential arising out of these is:

$$\begin{aligned}
V_{singlet} &= m_\chi^2 \chi^\dagger \chi + m_\gamma^2 \gamma^\dagger \gamma + \Lambda_1^s \{ \gamma^2 \chi + h.c. \} + \frac{\lambda_1^s}{2} [\chi^\dagger \chi]^2 + \frac{\lambda_2^s}{2} [\gamma^\dagger \gamma]^2 \\
&+ \frac{\lambda_3^s}{2} (\chi^\dagger \chi)(\gamma^\dagger \gamma) + \lambda_4^s \{ (\gamma^\dagger \chi)(\gamma^\dagger \chi) + h.c. \} ,
\end{aligned} \tag{B.1}$$

where the coefficient of the cubic term, Λ_1^s , carries the same dimension as mass while the λ_i^s are dimensionless.

B.2 $SU(2)_L$ Doublet Sector:

The $SU(2)_L$ doublet sector of the model has two fields $\Phi_{a,b}$ that are doublets of $S3$, in addition to α , β , and η which are $S3$ singlets. Among them, all fields except Φ_b and α ($\in \omega$ of Z_3) are invariant under Z_3 .

$$\begin{aligned}
V_{doublet} &= m_{\Phi_a}^2 \Phi_a^\dagger \Phi_a + m_{\Phi_b}^2 \Phi_b^\dagger \Phi_b + m_\eta^2 \eta^\dagger \eta + m_\alpha^2 \alpha^\dagger \alpha + m_\beta^2 \beta^\dagger \beta \\
&+ \frac{\lambda_1^d}{2} (\Phi_a^\dagger \Phi_a)^2 + \frac{\lambda_2^d}{2} (\Phi_b^\dagger \Phi_b)^2 + \frac{\lambda_3^d}{2} (\Phi_a^\dagger \Phi_a)(\Phi_b^\dagger \Phi_b) + \frac{\lambda_4^d}{2} (\Phi_a^\dagger \Phi_b)(\Phi_b^\dagger \Phi_a) \\
&+ \frac{\lambda_5^d}{2} (\Phi_a^\dagger \Phi_a)(\eta^\dagger \eta) + \frac{\lambda_6^d}{2} (\Phi_a^\dagger \Phi_a)(\alpha^\dagger \alpha) + \frac{\lambda_7^d}{2} (\Phi_a^\dagger \Phi_a)(\beta^\dagger \beta) + \frac{\lambda_8^d}{2} (\Phi_b^\dagger \Phi_b)(\alpha^\dagger \alpha) \\
&+ \frac{\lambda_9^d}{2} (\Phi_b^\dagger \Phi_b)(\beta^\dagger \beta) + \frac{\lambda_{10}^d}{2} (\Phi_b^\dagger \Phi_b)(\eta^\dagger \eta) + \frac{\lambda_{11}^d}{2} (\alpha^\dagger \alpha)^2 + \frac{\lambda_{12}^d}{2} (\alpha^\dagger \alpha)(\eta^\dagger \eta) \\
&+ \frac{\lambda_{13}^d}{2} (\alpha^\dagger \eta)(\eta^\dagger \alpha) + \frac{\lambda_{14}^d}{2} (\alpha^\dagger \alpha)(\beta^\dagger \beta) + \frac{\lambda_{15}^d}{2} (\eta^\dagger \eta)^2 + \frac{\lambda_{16}^d}{2} (\eta^\dagger \eta)(\beta^\dagger \beta) \\
&+ \lambda_{17}^d \{ (\Phi_a^\dagger \Phi_b)(\alpha^\dagger \eta) + h.c. \} + \frac{\lambda_{18}^d}{2} (\beta^\dagger \beta)^2 .
\end{aligned} \tag{B.2}$$

Leaving aside $S3$ properties for the moment, to which we return below, out of any $SU(2)$ doublet Φ one can construct two quartic invariants $(\Phi^\dagger \Phi)(\Phi^\dagger \Phi)$ and $(\Phi^\dagger \tau \Phi)(\Phi^\dagger \tau \Phi)$. Needless to say, this can be generalised to the case where several distinct $SU(2)$ doublets are involved. In order to avoid cluttering, in Eq. (B.2) we have displayed only the first combination for all quartic terms.

The quartic terms involving λ_1 to λ_4 in Eq. (B.2) are combinations of two pairs of $S3$ doublets. Each pair can combine in accordance to $2 \times 2 = 1 + 1' + 2$ resulting in three terms. The $S3$ invariant in the potential arises from a combination of the 1, $1'$, or 2 from one pair with the corresponding term from the other pair. Thus, for each such term of four $S3$ doublets, three possible singlet combinations exist (recall, Eq. (A.3)) and we have to keep an account of all of them. We elaborate on this using as an example the λ_1^d term which actually stands for a set of terms:

$$\frac{\lambda_1^d}{2} (\Phi_a^\dagger \Phi_a)^2 \rightarrow \lambda_{11}^d [(\Phi_1^\dagger \Phi_1) + (\Phi_2^\dagger \Phi_2)]^2 + \lambda_{11'}^d [(\Phi_1^\dagger \Phi_1) - (\Phi_2^\dagger \Phi_2)]^2 + \lambda_{12}^d [(\Phi_1^\dagger \Phi_2)(\Phi_2^\dagger \Phi_1) + (\Phi_2^\dagger \Phi_1)(\Phi_1^\dagger \Phi_2)] . \tag{B.3}$$

Substituting *vevs*, $\langle \Phi_1 \rangle = v_1$ and $\langle \Phi_2 \rangle = v_2$ and defining $\lambda_{11}^d + \lambda_{11'}^d = \frac{\lambda_{a1}^d}{2}$ and $2(\lambda_{11}^d - \lambda_{11'}^d + \lambda_{12}^d) = \frac{\lambda_{a2}^d}{2}$ we get:

$$\frac{\lambda_1^d}{2} (\Phi_a^\dagger \Phi_a)^2 \rightarrow \frac{\lambda_{a1}^d}{2} [(v_1^* v_1)^2 + (v_2^* v_2)^2] + \frac{\lambda_{a2}^d}{2} (v_1^* v_1)(v_2^* v_2) . \tag{B.4}$$

Similarly,

$$\frac{\lambda_2^d}{2} (\Phi_b^\dagger \Phi_b)^2 \longrightarrow \frac{\lambda_{b1}^d}{2} [(v_3^* v_3)^2 + (v_4^* v_4)^2] + \frac{\lambda_{b2}^d}{2} (v_3^* v_3)(v_4^* v_4) \quad (\text{B.5})$$

where, $\langle \Phi_3 \rangle = v_3$ and $\langle \Phi_4 \rangle = v_4$. Further,

$$\begin{aligned} \frac{\lambda_3^d}{2} [(\Phi_a^\dagger \Phi_a)(\Phi_b^\dagger \Phi_b)] &\rightarrow \lambda_{31}^d [(\Phi_1^\dagger \Phi_1 + \Phi_2^\dagger \Phi_2)(\Phi_3^\dagger \Phi_3 + \Phi_4^\dagger \Phi_4)] + \lambda_{31'}^d [(\Phi_1^\dagger \Phi_1 - \Phi_2^\dagger \Phi_2)(\Phi_3^\dagger \Phi_3 - \Phi_4^\dagger \Phi_4)] \\ &+ \lambda_{32}^d [(\Phi_1^\dagger \Phi_2)(\Phi_4^\dagger \Phi_3) + (\Phi_2^\dagger \Phi_1)(\Phi_3^\dagger \Phi_4)]. \end{aligned} \quad (\text{B.6})$$

Substituting the respective *vevs* and defining $\lambda_{31}^d + \lambda_{31'}^d = \frac{\lambda_{ab1}^d}{2}$, $\lambda_{31}^d - \lambda_{31'}^d = \frac{\lambda_{ab2}^d}{2}$ and $\lambda_{32}^d = \lambda_{ab3}^d$ we get;

$$\begin{aligned} \frac{\lambda_3^d}{2} [(\Phi_a^\dagger \Phi_a)(\Phi_b^\dagger \Phi_b)] &\longrightarrow \frac{\lambda_{ab1}^d}{2} [(v_1^* v_1)(v_3^* v_3) + (v_2^* v_2)(v_4^* v_4)] + \frac{\lambda_{ab2}^d}{2} [(v_1^* v_1)(v_4^* v_4) + (v_2^* v_2)(v_3^* v_3)] \\ &+ \lambda_{ab3}^d [(v_1^* v_2)(v_4^* v_3) + (v_2^* v_1)(v_3^* v_4)]. \end{aligned} \quad (\text{B.7})$$

In a similar fashion the λ_4^d term when expanded will lead to

$$\begin{aligned} \frac{\lambda_4^d}{2} [(\Phi_a^\dagger \Phi_b)(\Phi_b^\dagger \Phi_a)] &\longrightarrow \frac{\tilde{\lambda}_{ab1}^d}{2} [(v_1^* v_3)(v_3^* v_1) + (v_2^* v_4)(v_4^* v_2)] + \frac{\tilde{\lambda}_{ab2}^d}{2} [(v_1^* v_3)(v_4^* v_2) + (v_2^* v_4)(v_3^* v_1)] \\ &+ \tilde{\lambda}_{ab3}^d [(v_1^* v_4)(v_4^* v_1) + (v_2^* v_3)(v_3^* v_2)]. \end{aligned} \quad (\text{B.8})$$

Adding Eqs.(B.7) and Eq.(B.8) we get:

$$\begin{aligned} \frac{\lambda_3^d}{2} [(\Phi_a^\dagger \Phi_a)(\Phi_b^\dagger \Phi_b)] + \frac{\lambda_4^d}{2} [(\Phi_a^\dagger \Phi_b)(\Phi_b^\dagger \Phi_a)] &= \frac{\hat{\lambda}_{ab1}^d}{2} [(v_1^* v_1)(v_3^* v_3) + (v_2^* v_2)(v_4^* v_4)] \\ &+ \frac{\hat{\lambda}_{ab2}^d}{2} [(v_1^* v_1)(v_4^* v_4) + (v_2^* v_2)(v_3^* v_3)] \\ &+ \hat{\lambda}_{ab3}^d [(v_1^* v_2)(v_4^* v_3) + (v_2^* v_1)(v_3^* v_4)]; \end{aligned} \quad (\text{B.9})$$

where, $\frac{\hat{\lambda}_{ab1}^d}{2} \equiv \frac{\tilde{\lambda}_{ab1}^d}{2} + \frac{\lambda_{ab1}^d}{2}$, $\frac{\hat{\lambda}_{ab2}^d}{2} \equiv \tilde{\lambda}_{ab3}^d + \frac{\lambda_{ab2}^d}{2}$ and $\hat{\lambda}_{ab3}^d \equiv \frac{\tilde{\lambda}_{ab2}^d}{2} + \lambda_{ab3}^d$. Also, summing up the λ_{12}^d and λ_{13}^d terms lead to $\frac{\hat{\lambda}_{123}^d}{2} (v_\alpha^* v_\alpha)(v_\eta^* v_\eta)$, where $\hat{\lambda}_{123}^d \equiv \lambda_{12}^d + \lambda_{13}^d$.

B.3 $SU(2)_L$ Triplet Sector:

Both the $SU(2)_L$ triplets present in our model (Δ_L, ρ_L) that are responsible for Majorana mass generation of the left handed neutrinos happen to be $S3$ invariants and differ only in their Z_3 properties i.e., $\Delta_L(1)$ and $\rho_L(\omega)$.

$$\begin{aligned} V_{\text{triplet}} &= m_{\Delta_L}^2 \Delta_L^\dagger \Delta_L + m_{\rho_L}^2 \rho_L^\dagger \rho_L + \frac{\lambda_1^t}{2} [\Delta_L^\dagger \Delta_L]^2 + \frac{\lambda_2^t}{2} [\rho_L^\dagger \rho_L]^2 + \frac{\lambda_3^t}{2} (\Delta_L^\dagger \Delta_L)(\rho_L^\dagger \rho_L) \\ &+ \frac{\lambda_4^t}{2} (\Delta_L^\dagger \rho_L)(\rho_L^\dagger \Delta_L) + \frac{\lambda_5^t}{2} (\Delta_L \rho_L)(\Delta_L \rho_L)^\dagger. \end{aligned} \quad (\text{B.10})$$

It is noteworthy that when we write the minimized potential in terms of the vacuum expectation values, the λ_3^t , λ_4^t and λ_5^t terms will be providing the same contribution as far as potential minimization is concerned. Thus we can club these couplings together as $\lambda_{345}^t \equiv \lambda_3^t + \lambda_4^t + \lambda_5^t$.

B.4 Inter-sector terms:

So far we have listed those terms in the potential which arise from scalars of any specific $SU(2)_L$ behaviour – singlets, doublets, or triplets. In addition, there can be terms which couple one of these sectors to another. Since the vacuum expectation values of the singlet scalars are the largest we only consider here the couplings of this sector to the others. The $SU(2)_L$ triplet sector vev is very small and we drop the doublet-triplet cross-sector couplings.

B.4.1 $SU(2)_L$ Singlet-Doublet cross-sector:

Couplings between the $SU(2)_L$ singlet and doublet scalars in the potential give rise to the terms:

$$\begin{aligned}
V_{ds} = & \Lambda_1^{ds} \left[(\Phi_b^\dagger \Phi_a)_{1'} \gamma + h.c. \right] + \Lambda_2^{ds} \left[(\Phi_b^\dagger \Phi_a)_1 \chi + h.c. \right] + \Lambda_3^{ds} \left[(\alpha^\dagger \eta) \chi + h.c. \right] \\
& + \frac{\lambda_1^{ds}}{2} (\Phi_a^\dagger \Phi_a) (\chi^\dagger \chi) + \frac{\lambda_2^{ds}}{2} (\Phi_a^\dagger \Phi_a) (\gamma^\dagger \gamma) + \frac{\lambda_3^{ds}}{2} (\Phi_b^\dagger \Phi_b) (\chi^\dagger \chi) + \frac{\lambda_4^{ds}}{2} (\Phi_b^\dagger \Phi_b) (\gamma^\dagger \gamma) \\
& + \frac{\lambda_5^{ds}}{2} (\alpha^\dagger \alpha) (\chi^\dagger \chi) + \frac{\lambda_6^{ds}}{2} (\alpha^\dagger \alpha) (\gamma^\dagger \gamma) + \frac{\lambda_7^{ds}}{2} (\eta^\dagger \eta) (\chi^\dagger \chi) + \frac{\lambda_8^{ds}}{2} (\eta^\dagger \eta) (\gamma^\dagger \gamma) \\
& + \lambda_9^{ds} \left[(\Phi_a^\dagger \Phi_b) \chi^2 + h.c. \right] + \lambda_{10}^{ds} \left[(\Phi_a^\dagger \Phi_b) \gamma^2 + h.c. \right] + \lambda_{11}^{ds} \left[(\eta^\dagger \alpha) \chi^2 + h.c. \right] + \lambda_{12}^{ds} \left[(\eta^\dagger \alpha) \gamma^2 + h.c. \right] \\
& + \lambda_{13}^{ds} \left[(\Phi_a^\dagger \Phi_b)_{1'} (\chi \gamma) + h.c. \right] + \frac{\lambda_{14}^{ds}}{2} (\beta^\dagger \beta) (\chi^\dagger \chi) + \frac{\lambda_{15}^{ds}}{2} (\beta^\dagger \beta) (\gamma^\dagger \gamma) .
\end{aligned} \tag{B.11}$$

B.4.2 $SU(2)_L$ Singlet-Triplet cross-sector:

The terms in the potential which arise from couplings between the $SU(2)_L$ singlet and triplet scalars are:

$$\begin{aligned}
V_{ts} = & \Lambda_1^{ts} \left[(\rho_L^\dagger \Delta_L) \chi + h.c. \right] + \frac{\lambda_1^{ts}}{2} (\Delta_L^\dagger \Delta_L) (\chi^\dagger \chi) + \frac{\lambda_2^{ts}}{2} (\Delta_L^\dagger \Delta_L) (\gamma^\dagger \gamma) + \frac{\lambda_3^{ts}}{2} (\rho_L^\dagger \rho_L) (\chi^\dagger \chi) \\
& + \frac{\lambda_4^{ts}}{2} (\rho_L^\dagger \rho_L) (\gamma^\dagger \gamma) + \lambda_5^{ts} \left\{ (\Delta_L^\dagger \rho_L) \chi^2 + h.c. \right\} + \lambda_6^{ts} \left\{ (\Delta_L^\dagger \rho_L) \gamma^2 + h.c. \right\} .
\end{aligned} \tag{B.12}$$

B.5 The minimization conditions:

The vevs of the scalar fields are given in Table 3. Using these:

$SU(2)_L$ singlets: $\langle \gamma^0 \rangle = u_\gamma$ and $\langle \chi^0 \rangle = u_\chi$.

$SU(2)_L$ doublets: $\langle \Phi_a \rangle = \begin{pmatrix} 0 & v_1 \\ 0 & v_2 \end{pmatrix}$, $\langle \Phi_b \rangle = \begin{pmatrix} 0 & v_3 \\ 0 & v_4 \end{pmatrix}$, $\langle \eta \rangle = v_\eta (0 \ 1)$, $\langle \alpha \rangle = v_\alpha (0 \ 1)$ and $\langle \beta \rangle = v_\beta (1 \ 0)$.

Recall that from the structure of the charged lepton mass matrix Eq. (13) requires $v_2/v_1 = v_4/v_3 = A$ where the real quantity $A = m_\mu/m_\tau$. We often also need $B \equiv (1 + A^2)$.

$SU(2)_L$ triplets: $\langle \rho_L^0 \rangle = v_\rho$ and $\langle \Delta_L^0 \rangle = v_\Delta$.

B.5.1 $SU(2)_L$ Singlet sector:

$$\frac{\partial V_{singlet}|_{min}}{\partial u_\chi^*} = 0 \Rightarrow u_\chi [m_\chi^2 + \lambda_1^s u_\chi^* u_\chi] + \Lambda_1^s (u_\gamma^*)^2 + u_\gamma \left[\frac{\lambda_3^s}{2} u_\chi u_\gamma^* + 2\lambda_4^s u_\chi^* u_\gamma \right] = 0, \quad (\text{B.13})$$

and

$$\frac{\partial V_{singlet}|_{min}}{\partial u_\gamma^*} = 0 \Rightarrow u_\gamma [m_\gamma^2 + \lambda_2^s u_\gamma^* u_\gamma] + 2\Lambda_1^s (u_\gamma^* u_\chi^*) + u_\chi \left[\frac{\lambda_3^s}{2} u_\gamma u_\chi^* + 2\lambda_4^s u_\gamma^* u_\chi \right] = 0. \quad (\text{B.14})$$

B.5.2 $SU(2)_L$ Doublet sector:

Define $V_{\mathcal{D}} = V_{doublet} + V_{ds}$.

$$\begin{aligned} \frac{\partial V_{\mathcal{D}}|_{min}}{\partial v_\alpha^*} &= v_\alpha \left[m_\alpha^2 + \frac{\lambda_6^d}{2} (v_1^* v_1) B + \frac{\lambda_8^d}{2} (v_3^* v_3) B + \lambda_{11}^d (v_\alpha^* v_\alpha) + \frac{\hat{\lambda}_{123}^d}{2} (v_\eta^* v_\eta) + \lambda_{14}^d (v_\beta^* v_\beta) \right] \\ &+ v_\alpha \left[\frac{\lambda_5^{ds}}{2} (u_\chi^* u_\chi) + \frac{\lambda_6^{ds}}{2} (u_\gamma^* u_\gamma) \right] + v_\eta \left[\lambda_{17}^d (v_1^* v_3) B + \Lambda_3^{ds} u_\chi + \lambda_{11}^{ds} (u_\chi^*)^2 + \lambda_{12}^{ds} (u_\gamma^*)^2 \right] = 0. \end{aligned} \quad (\text{B.15})$$

$$\begin{aligned} \frac{\partial V_{\mathcal{D}}|_{min}}{\partial v_\beta^*} &= v_\beta \left[m_\beta^2 + \frac{\lambda_7^d}{2} (v_1^* v_1) B + \frac{\lambda_9^d}{2} (v_3^* v_3) B + \frac{\lambda_{14}^d}{2} (v_\alpha^* v_\alpha) + \frac{\lambda_{16}^d}{2} (v_\eta^* v_\eta) + \lambda_{18}^d (v_\beta^* v_\beta) \right] \\ &+ v_\beta \left[\frac{\lambda_{14}^{ds}}{2} (u_\chi^* u_\chi) + \frac{\lambda_{15}^{ds}}{2} (u_\gamma^* u_\gamma) \right] = 0. \end{aligned} \quad (\text{B.16})$$

$$\begin{aligned} \frac{\partial V_{\mathcal{D}}|_{min}}{\partial v_\eta^*} &= v_\eta \left[m_\eta^2 + \frac{\lambda_5^d}{2} (v_1^* v_1) B + \frac{\lambda_{10}^d}{2} (v_3^* v_3) B + \frac{\hat{\lambda}_{123}^d}{2} (v_\alpha^* v_\alpha) + \lambda_{15}^d (v_\eta^* v_\eta) + \frac{\lambda_{16}^d}{2} (v_\beta^* v_\beta) \right] \\ &+ v_\eta \left[\frac{\lambda_7^{ds}}{2} (u_\chi^* u_\chi) + \frac{\lambda_8^{ds}}{2} (u_\gamma^* u_\gamma) \right] + v_\alpha \left[\lambda_{17}^d (v_3^* v_1) B + \Lambda_3^{ds} u_\chi^* + \lambda_{11}^{ds} (u_\chi)^2 + \lambda_{12}^{ds} (u_\gamma)^2 \right] \\ &= 0. \end{aligned} \quad (\text{B.17})$$

$$\begin{aligned} \frac{\partial V_{\mathcal{D}}|_{min}}{\partial v_1^*} &= v_1 \left[m_{\Phi_a}^2 + (v_1^* v_1) \left(\lambda_{a_1}^d + A^2 \frac{\lambda_{a_2}^d}{2} \right) + (v_3^* v_3) \left(\frac{\hat{\lambda}_{ab_1}^d}{2} + A^2 \frac{\hat{\lambda}_{ab_2}^d}{2} + A^2 \hat{\lambda}_{ab_3}^d \right) \right] \\ &+ v_1 \left[\left\{ \frac{\lambda_5^d}{2} (v_\eta^* v_\eta) + \frac{\lambda_6^d}{2} (v_\alpha^* v_\alpha) + \frac{\lambda_7^d}{2} (v_\beta^* v_\beta) \right\} + \left\{ \frac{\lambda_1^{ds}}{2} (u_\chi^* u_\chi) + \frac{\lambda_2^{ds}}{2} (u_\gamma^* u_\gamma) \right\} \right] \\ &+ v_3 \left[\left\{ \lambda_{17}^d (v_\alpha^* v_\eta) \right\} + \left\{ \Lambda_1^{ds} u_\gamma^* + \Lambda_2^{ds} u_\chi^* + \lambda_9^{ds} (u_\chi)^2 + \lambda_{10}^{ds} (u_\gamma)^2 + \lambda_{13}^{ds} (u_\chi u_\gamma) \right\} \right] \\ &= 0. \end{aligned} \quad (\text{B.18})$$

$$\begin{aligned}
\frac{\partial V_{\mathcal{D}}|_{min}}{\partial v_2^*} &= Av_1 \left[m_{\Phi_a}^2 + (v_1^* v_1) \left(A^2 \lambda_{a1}^d + \frac{\lambda_{a2}^d}{2} \right) + (v_3^* v_3) \left(A^2 \frac{\hat{\lambda}_{ab1}^d}{2} + \frac{\hat{\lambda}_{ab2}^d}{2} + \hat{\lambda}_{ab3}^d \right) \right] \\
&+ Av_1 \left[\left\{ \frac{\lambda_5^d}{2} (v_\eta^* v_\eta) + \frac{\lambda_6^d}{2} (v_\alpha^* v_\alpha) + \frac{\lambda_7^d}{2} (v_\beta^* v_\beta) \right\} + \left\{ \frac{\lambda_1^{ds}}{2} (u_\chi^* u_\chi) + \frac{\lambda_2^{ds}}{2} (u_\gamma^* u_\gamma) \right\} \right] \\
&+ Av_3 \left[\left\{ \lambda_{17}^d (v_\alpha^* v_\eta) \right\} + \left\{ -\Lambda_1^{ds} u_\gamma^* + \Lambda_2^{ds} u_\chi^* + \lambda_9^{ds} (u_\chi)^2 + \lambda_{10}^{ds} (u_\gamma)^2 - \lambda_{13}^{ds} (u_\chi u_\gamma) \right\} \right] \\
&= 0.
\end{aligned} \tag{B.19}$$

$$\begin{aligned}
\frac{\partial V_{\mathcal{D}}|_{min}}{\partial v_3^*} &= v_3 \left[m_{\Phi_b}^2 + (v_3^* v_3) \left(\lambda_{b1}^d + A^2 \frac{\lambda_{b2}^d}{2} \right) + (v_1^* v_1) \left(\frac{\hat{\lambda}_{ab1}^d}{2} + A^2 \frac{\hat{\lambda}_{ab2}^d}{2} + A^2 \hat{\lambda}_{ab3}^d \right) \right] \\
&+ v_3 \left[\left\{ \frac{\lambda_8^d}{2} (v_\alpha^* v_\alpha) + \frac{\lambda_9^d}{2} (v_\beta^* v_\beta) + \frac{\lambda_{10}^d}{2} (v_\eta^* v_\eta) \right\} + \left\{ \frac{\lambda_3^{ds}}{2} (u_\chi^* u_\chi) + \frac{\lambda_4^{ds}}{2} (u_\gamma^* u_\gamma) \right\} \right] \\
&+ v_1 \left[\left\{ \lambda_{17}^d (v_\eta^* v_\alpha) \right\} + \left\{ \Lambda_1^{ds} u_\gamma + \Lambda_2^{ds} u_\chi + \lambda_9^{ds} (u_\chi^*)^2 + \lambda_{10}^{ds} (u_\gamma^*)^2 + \lambda_{13}^{ds} (u_\chi^* u_\gamma^*) \right\} \right] \\
&= 0.
\end{aligned} \tag{B.20}$$

$$\begin{aligned}
\frac{\partial V_{\mathcal{D}}|_{min}}{\partial v_4^*} &= Av_3 \left[m_{\Phi_b}^2 + (v_3^* v_3) \left(A^2 \lambda_{b1}^d + \frac{\lambda_{b2}^d}{2} \right) + (v_1^* v_1) \left(A^2 \frac{\hat{\lambda}_{ab1}^d}{2} + \frac{\hat{\lambda}_{ab2}^d}{2} + \hat{\lambda}_{ab3}^d \right) \right] \\
&+ Av_3 \left[\left\{ \frac{\lambda_8^d}{2} (v_\alpha^* v_\alpha) + \frac{\lambda_9^d}{2} (v_\beta^* v_\beta) + \frac{\lambda_{10}^d}{2} (v_\eta^* v_\eta) \right\} + \left\{ \frac{\lambda_3^{ds}}{2} (u_\chi^* u_\chi) + \frac{\lambda_4^{ds}}{2} (u_\gamma^* u_\gamma) \right\} \right] \\
&+ Av_1 \left[\left\{ \lambda_{17}^d (v_\eta^* v_\alpha) \right\} + \left\{ -\Lambda_1^{ds} u_\gamma + \Lambda_2^{ds} u_\chi + \lambda_9^{ds} (u_\chi^*)^2 + \lambda_{10}^{ds} (u_\gamma^*)^2 - \lambda_{13}^{ds} (u_\chi^* u_\gamma^*) \right\} \right] \\
&= 0.
\end{aligned} \tag{B.21}$$

B.5.3 $SU(2)_L$ Triplet sector:

Define $V_{\mathcal{F}} = V_{triplet} + V_{ts}$.

$$\begin{aligned}
\frac{\partial V_{\mathcal{F}}|_{min}}{\partial v_\Delta^*} &= v_\Delta \left[\left\{ m_{\Delta_L}^2 + \lambda_1^t (v_\Delta^* v_\Delta) + \frac{\lambda_{345}^t}{2} (v_\rho^* v_\rho) \right\} + \left\{ \frac{\lambda_1^{ts}}{2} (u_\chi^* u_\chi) + \frac{\lambda_2^{ts}}{2} (u_\gamma^* u_\gamma) \right\} \right] \\
&+ v_\rho \left[\Lambda_1^{ts} u_\chi^* + \lambda_5^{ts} u_\chi^2 + \lambda_6^{ts} u_\gamma^2 \right] = 0.
\end{aligned} \tag{B.22}$$

$$\begin{aligned}
\frac{\partial V_{\mathcal{F}}|_{min}}{\partial v_\rho^*} &= v_\rho \left[\left\{ m_{\rho_L}^2 + \lambda_2^t (v_\rho^* v_\rho) + \frac{\lambda_{345}^t}{2} (v_\Delta^* v_\Delta) \right\} + \left\{ \frac{\lambda_3^{ts}}{2} (u_\chi^* u_\chi) + \frac{\lambda_4^{ts}}{2} (u_\gamma^* u_\gamma) \right\} \right] \\
&+ v_\Delta \left[\Lambda_1^{ts} u_\chi + \lambda_5^{ts} (u_\chi^*)^2 + \lambda_6^{ts} (u_\gamma^*)^2 \right] = 0.
\end{aligned} \tag{B.23}$$

References

- [1] See, for example, P. F. Harrison and W. G. Scott, Phys. Lett. B **557**, 76 (2003) [hep-ph/0302025].
- [2] S. L. Chen, M. Frigerio and E. Ma, Phys. Rev. D **70**, 073008 (2004) Erratum: [Phys. Rev. D **70**, 079905 (2004)] [hep-ph/0404084]; E. Ma, Phys. Rev. D **61**, 033012 (2000) [hep-ph/9909249].
- [3] A sampling is W. Grimus and L. Lavoura, JHEP **0508**, 013 (2005) [hep-ph/0504153]; R. Jora, J. Schechter and M. Naeem Shahid, Phys. Rev. D **80**, 093007 (2009) Erratum: [Phys. Rev. D **82**, 079902 (2010)] [arXiv:0909.4414 [hep-ph]]; Z. z. Xing, D. Yang and S. Zhou, Phys. Lett. B **690**, 304 (2010) [arXiv:1004.4234 [hep-ph]]; T. Teshima and Y. Okumura, Phys. Rev. D **84**, 016003 (2011) [arXiv:1103.6127 [hep-ph]]; S. Dev, S. Gupta and R. R. Gautam, Phys. Lett. B **702**, 28 (2011) [arXiv:1106.3873 [hep-ph]]; S. Zhou, Phys. Lett. B **704**, 291 (2011) [arXiv:1106.4808 [hep-ph]]; R. Jora, J. Schechter and M. N. Shahid, Int. J. Mod. Phys. A **28**, 1350028 (2013) [arXiv:1210.6755 [hep-ph]]; H. B. Benaoum, Phys. Rev. D **87**, 073010 (2013) [arXiv:1302.0950 [hep-ph]].
- [4] S. Morisi, hep-ph/0605167; M. Tanimoto and T. Yanagida, Phys. Lett. B **633**, 567 (2006) [hep-ph/0511336]; S. Gupta, C. S. Kim and P. Sharma, Phys. Lett. B **740**, 353 (2015) [arXiv:1408.0172 [hep-ph]].
- [5] A. E. C. Hernandez, E. C. Mur and R. Martinez, Phys. Rev. D **90**, 073001 (2014) [arXiv:1407.5217 [hep-ph]]; V. V. Vien and H. N. Long, Zh. Eksp. Teor. Fiz. **145**, 991 (2014) J. Exp. Theor. Phys. **118**, 869 (2014) [arXiv:1404.6119 [hep-ph]]; E. Ma and R. Srivastava, Phys. Lett. B **741**, 217 (2015) [arXiv:1411.5042 [hep-ph]]; D. Meloni, S. Morisi and E. Peinado, J. Phys. G **38**, 015003 (2011) [arXiv:1005.3482 [hep-ph]]; A. E. Carcamo Hernandez, I. de Medeiros Varzielas and E. Schumacher, Phys. Rev. D **93**, 016003 (2016) [arXiv:1509.02083 [hep-ph]]; A. E. Carcamo Hernandez, I. de Medeiros Varzielas and N. A. Neill, Phys. Rev. D **94**, 033011 (2016) [arXiv:1511.07420 [hep-ph]]; D. Das, U. K. Dey and P. B. Pal, Phys. Lett. B **753**, 315 (2016) [arXiv:1507.06509 [hep-ph]]; R. N. Mohapatra, S. Nasri and H. B. Yu, Phys. Lett. B **639**, 318 (2006) [hep-ph/0605020].
- [6] F. Feruglio and Y. Lin, Nucl. Phys. B **800**, 77 (2008) [arXiv:0712.1528 [hep-ph]].
- [7] For the present status of θ_{13} see presentations from Double Chooz, RENO, Daya Bay, and T2K at Neutrino 2016 (<http://neutrino2016.iopconfs.org/programme>).
- [8] S. Pramanick and A. Raychaudhuri, Phys. Rev. D **93**, 033007 (2016) [arXiv:1508.02330 [hep-ph]].
- [9] S. Pramanick and A. Raychaudhuri, Phys. Lett. B **746**, 237 (2015) [arXiv:1411.0320 [hep-ph]]; Int. J. Mod. Phys. A **30**, 1530036 (2015) [arXiv:1504.01555 [hep-ph]].
- [10] B. Brahmachari and A. Raychaudhuri, Phys. Rev. D **86**, 051302 (2012) [arXiv:1204.5619 [hep-ph]]; S. Pramanick and A. Raychaudhuri, Phys. Rev. D **88**, 093009 (2013) [arXiv:1308.1445 [hep-ph]].
- [11] J. Kubo, A. Mondragon, M. Mondragon and E. Rodriguez-Jauregui, Prog. Theor. Phys. **109**, 795 (2003) Erratum: [Prog. Theor. Phys. **114**, 287 (2005)] [hep-ph/0302196]; S. Kaneko, H. Sawanaka, T. Shingai, M. Tanimoto and K. Yoshioka, Prog. Theor. Phys. **117**, 161 (2007) [hep-ph/0609220].
- [12] M. C. Gonzalez-Garcia, M. Maltoni, J. Salvado and T. Schwetz, JHEP **1212**, 123 (2012) [arXiv:1209.3023v3 [hep-ph]], NuFIT 2.1 (2016).

- [13] D. V. Forero, M. Tortola and J. W. F. Valle, Phys. Rev. D **86**, 073012 (2012) [arXiv:1205.4018 [hep-ph]].
- [14] K. Abe et al. (T2K collaboration), arXiv:1502.01550v2 [hep-ex] (see Fig. 37).
- [15] P. Adamson et al. (NOVA collaboration), arXiv:1601.05022v2 [hep-ex].
- [16] M. Haag [KATRIN Collaboration], PoS EPS **-HEP2013**, 518 (2013).
- [17] See, for example, G. Drexlin, V. Hannen, S. Mertens and C. Weinheimer, Adv. High Energy Phys. **2013**, 293986 (2013) [arXiv:1307.0101 [physics.ins-det]].